Heliyon 8 (2022) e11190

Contents lists available at ScienceDirect

Heliyon

journal homepage: www.cell.com/heliyon

Research article

BNIP3 enhances pancreatic cancer cell migration and proliferation via modulating autophagy under hypoxia

Hongmei Li [a,1], Can Zhang [b,1], Qiong Zhang [c], Jiezhi Jia [c], Xiaojiao Wang [a,*]

[a] Department of Oncology and Southwest Cancer Center, Southwest Hospital, Third Military Medical University (Army Medical University), Chongqing, 400038, China
[b] Department of Plastic Surgery, Southwest Hospital, Third Military Medical University (Army Medical University), Chongqing, 400038, China
[c] Institute of Burn Research, State Key Laboratory of Trauma, Burns and Combined Injury, Southwest Hospital, Third Military Medical University (Army Medical University), Chongqing, 400038, China

ARTICLE INFO

Keywords:
BNIP3
Autophagy
ERK1/2
Pancreatic ductal adenocarcinoma
Hypoxia

ABSTRACT

Chemotherapy and immunotherapy for pancreatic ductal adenocarcinoma (PDAC) have limited success for the intricated surrounding cancer microenvironment. Hypoxic microenvironment in PDAC causes the activation of multiple different molecules and signaling pathways compared with normoxia. We studied the roles of BNIP3 for the migration and proliferation of PDAC and Panc1 cells *in vitro*. In the present study, we found that BNIP3 expression was elevated and enhanced the migration and proliferation of CFPAC-1 and Panc1 cells under hypoxia. The upregulation of BNIP3 was important for the autophagic activation, while inhibition of autophagy with siRNA targeting Atg5 and Atg7 impaired the hypoxia-induced cell migration and proliferation. Additionally, blocking ERK1/2 mitogen-activated protein kinase (MAPK) signaling with PD98058 significantly down-regulated BNIP3 expression, autophagic activation, as well as the migration and proliferation of CFPAC-1 and Panc1 cells under hypoxia. Collectively, our results here uncover a hitherto unknown hypoxia-BNIP3-autophagy axis in modulating the migration and proliferation and provide a potential intriguing drug target for the therapy of PDAC.

1. Introduction

Pancreatic ductal adenocarcinoma (PDAC) remains an aggressive malignancy with a median survival about 6 months and the 5-year survival approximately 9% [1, 2]. PDAC is considered to be the second leading cause of cancer deaths within the next decade due to the lack of improved outcomes. Its intractability is mainly resulted from the late diagnosis, early dissemination of metastases, a paucity of specific and sensitive biomarkers, as well as the resistance to chemotherapy, radiotherapy, and even immunotherapy, which is resulted from inherent intratumor heterogeneity and a highly desmoplastic and immunosuppressive tumor microenvironment (TME) [3, 4].

Hypoxia, one of the most important TME, is a hallmark of many solid tumors that is related to the poor prognosis, treatment resistance, and elevated invasion and metastasis [5]. Hypoxia is clinically identified in the PDAC [6], and the investigation of orthotopic patient-derived xenografts (PDX) and genetically engineered mouse models (GEMM) indicates the correlation between hypoxia TME and the rapid tumor progression and metastasis. Intratumoral hypoxia leads to the upregulation of BNIP3 (Bcl-2 and adenovirus E1B 19-kDa interacting protein 3) [7], one of the known downstream targets of HIF1α (hypoxia-inducible factor 1 subunit alpha) [8]. BNIP3, a BH3-only protein that belongs to the Bcl-2 family, is proved with an emerging role in cell apoptosis and autophagy. Recent studies highlight a critical role for BNIP3 in carcinogenesis, such as laryngeal cancer, gastric cancer, glioma, melanoma, and hepatocellular carcinoma [9, 10, 11, 12]. However, a considerable debate still remain underlying the cellular processes and mechanisms regulated by BNIP3 in cancer cells. Moreover, whether and how BNIP3 regulates the progression and dissemination of PDAC cell remains largely unclear.

Autophagy is one of the resistance mechanism in tumor therapy that promotes cell survival in adverse environments, although the uncontrolled autophagy can promote apoptosis [13]. There are three types of autophagy, i.e. macroautophagy, chaperone-mediated autophagy, and microautophagy. Macroautophagy (hereafter referred to as autophagy) is indicated as the main autophagy process activated when cells suffering from nutrient insufficiency and hypoxia [14]. Previous studies have shown that autophagy is activated when the pancreas is invaded by the intravascular pancreatic neoplasia [15]. Additionally, the PDAC cells

* Corresponding author.
E-mail address: wangxiaojiao_tmmu@163.com (X. Wang).
[1] These authors contributed equally to this work.

https://doi.org/10.1016/j.heliyon.2022.e11190
Received 13 February 2022; Received in revised form 25 June 2022; Accepted 17 October 2022

have been demonstrated to rely on autophagy for nutrients and energy to survive in vitro [16]. A recent study suggests that autophagic flux can affect the immunogenicity of PDAC cells and that inhibiting autophagy can improve the sensitivity of PDAC cells to immunotherapy [17]. Thus autophagy acts a vital role for the occurrence, progession, and treatment.

Here, we set out to determine whether the BNIP3-induced autophagy impinges on the hypoxia response in PDAC cells. Indeed, our results show that BNIP3 up-regulates, mediates cell autophagy, and enhances the migration and proliferation of CFPAC-1 cells under hypoxia. In addition, we provide evidence that ERK1/2 MAPK signaling is significant activated and enhances BNIP3-mediated autophagy in CFPAC-1 cells under hypoxia. Inhibition of ERK1/2 signaling suppressed the migration, as well as the proliferation of CFPAC-1 cells under hypoxia. We conclude that hypoxic TME promotes the migration and proliferation of pancreatic cancer cell via modulating the BNIP3-autophagy axis with the involvement of ERK1/2 signaling pathway.

2. Materials and methods

2.1. Cells culture

The human pancreatic cell line CFPAC-1 obtained from American Type Culture Collection (ATCC, Manassas, Virginia, USA) was grown in IMDM (HyClone, Logan, Utah, USA) containing 10% fetal bovine serum (FBS; HyClone; GE Healthcare Life Sciences) and 1% streptomycin/penicillin (Beyotime). Panc1 cell obtained from ATCC was cultured in DMEM (Gibco, USA) containing 10% fetal bovine serum (FBS; HyClone; GE Healthcare Life Sciences) and 1% streptomycin/penicillin (Beyotime). Conventionally, the cells were incubated at 37 °C in an atmosphere containing 5% CO_2.

2.2. Hypoxia exposure

The Forma Series II Water Jacket CO_2 incubator (model: 3131; Thermo Scientific) was applied for the hypoxic conditions of 1% O_2, 5% CO_2 and 93% N_2, as well as the required temperature (37 °C) and O_2 level with a constant flow of nitrogen. An ERK1/2 inhibitor PD98059 was purchased from MedChem Express (HY-12028, 10 μM) was added to the cells and incubated for 1 h prior to hypoxic treatment.

2.3. Scratched wound healing assay

Cell monolayers cultured in 6-well plates were scratched by a 100-μL plastic pipette tip after incubating for 2 h with mitomycin-C (S8146, Selleck, 5 μg/mL) to inhibit the proliferation. Healing process of the wound was monitored under an inverted light microscope (Olympus, Japan). The wound-closure rate (%) was measured by NIH ImageJ software (http://rsb.info.nih.gov/ij/), which indicated the potential of cell migration.

2.4. Single cell motility assay and quantitative analysis

The cells were cultured at a density of $0.5 \times 10^4/cm^2$ in 24-well plates. Then time-lapse imaging was conducted with a Zeiss imaging system (Carl Zeiss Meditec, Jena, Germany) in a temperature- and CO_2-controlled chamber. The images were taken every 10 min for 3 h. The cells' trajectories were obtained using NIH ImageJ software by tracing the position of cell nucleus. The velocity of single cell movement (μm/min) was defined as the accumulated distance (μm) of the trajectories dividing by time (min).

2.5. Cell proliferation assay

5-Ethynyl-2'-deoxyuridine (EdU), a thymidine analog, was incorporated to label cells undergoing DNA replication. EdU-positive rate of cells was applied to evaluate the proliferative ability, as determined by EdU staining with the Click-iT™ EdU kit according to the manufacturer's instructions (BCK488-IV-IM-S, Sigma, USA) [18]. The Leica Confocal Microscope (SP5, Leica Microsystems, Germany) was used for capturing the fluorescent images. The Cell Counting Kit-8 (CCK-8, Genview, USA) assay was conducted refering to the manufacturer's instructions.

2.6. Lentivirus infection and small interfering RNA (siRNA) transfection

For the construction of stable cell line, BNIP3-overexpressing lentivirus (AdBNIP3) or the corresponding control lentivirus (AdNC) (Table S1) were obtained from the GeneChem Company (Shanghai, China) and used according to the manufacturer's instructions. The siRNAs, purchased from GenePharma Company (Shanghai, China), were transfected into cells for the interfering of BNIP3, Atg5 or Atg7 (Table S1) with lipofectamine 2000 (11668027, Invitrogen) according to the manufacturer's protocol.

2.7. Western blot analysis

Whole cell extracts were prepared in the RIPA lysis buffer (P0013, Beyotime) and then centrifuged (14,000 rpm, 4 °C) for 15 min. The supernatants were obtained and protein concentrations were tested with Bradford Protein Quantification Kit (500-0205, Bio-Rad Laboratories). The protein samples were loaded and separated by 8–12% SDS-PAGE, then transferred to PVDF membrane (Millipore). Tris-buffered saline with 0.1% Tween containing 5% non-fat milk was used to block the membranes for 2 h at room temperature. Then the membranes were incubated with the primary antibodies targeting BNIP3 (ab10433, Abcam, 1:1000), LC3B (L7543, Sigma, 1:5000), Atg5 (12994, Cell Signaling Technology, 1:1000), ERK1/2 (4695, Cell Signaling Technology, 1:1000), phosphorylated ERK1/2 (p-ERK1/2; 4370, Cell Signaling Technology, 1:1000), P62 (88588, Cell Signaling Technology, 1:1000) and β-actin (ACTB, HRP-66009, Proteintech, 1:2000) overnight at 4 °C. Then the corresponding secondary HRP–conjugated antibodies (1:5000) were incubated for 2 h at room temperature. The blots were visualized with the ChemiDoc XRS System (Bio-Rad Laboratories) using the enhanced chemiluminescence reagent (K-12045-D10, Advansta).

2.8. Immunoprecipitation (IP)

To test the interaction between BNIP3 and LC3, whole cell extracts were collected in the lysis buffer (Beyotime, P0013) and centrifuged at 14,000 g for 15 min. The supernatants were obtained and incubated with 2 μg of anti-LC3B (L7543, Sigma), anti-BNIP3 (ab10433, Abcam) at 4 °C for 8 h, then precipitated with the Protein A/G-Sepharose (sc-2003, Santa Cruz Biotechnology) overnight at 4 °C. The binding proteins were detected using western blotting. The denatured IgG light chain of the primary antibodies used for IP runs at about 25 kDa on the subsequent blotting, which may obscure the bands of BNIP3 (26 kDa). An secondary antibody specific for IgG heavy-chain was used to resolve this problem.

2.9. Recombinant adenovirus construction and transduction

The mRFP-GFP-LC3, Ad-Dsred-Mito (marking the mitochondrial) and Ad-GFP-LC3 (marking the autophagosome) adenovirus were obtained from the Hanbio Biotechnology (Shanghai, China) to detect autophagy flux and mitophagy, respectively. The cells were cultured on glass coverslips in 24-well plates and then transfected with these adenovirus overnight before the corresponding treatment. The fluorescent images were captured by a Leica Confocal Microscope (SP5, Leica Microsystems, Germany).

2.10. Immunofluorescence staining

After corresponding treatments, the CFPAC-1 cells were fixed with 4% paraformaldehyde (PFA) for 20 min after being rinsed twice with

cold phosphate buffer saline (PBS). Subsequently, the cells were incubated with the mouse anti-BNIP3 (ab10433, Abcam, 1:1000) and/or rabbit anti-LC3B (L7543, Sigma, 1:5000) at 4 °C overnight, washed 3 times with cold PBS, and then stained with the secondary antibodies: Alexa Fluor 488-conjugated goat anti-rabbit IgG antibody and Alexa Fluor 561-conjugated goat anti-mouse IgG antibody (Invitrogen, 1:100) for 1 h at 37 °C. Nuclei were counterstained with 4', 6-diamidino-2-phenylindole (DAPI) (Sigma, USA) for 5 min before imaging with a Leica Confocal Microscope (SP5, Leica Microsystems, Germany).

2.11. Statistical analysis

All these data were analyzed using SPSS statistics 22.0 software and presented as means ± SEM. Independent t test was used to explore the difference between two groups. One-way analysis of variance (ANOVA with Post Hoc LSD) were applied to evaluate the difference among three or more groups in all measured parameters. A $p < 0.05$ was considered as the statistical significance.

3. Results

3.1. BNIP3 enhanced the migration and proliferation of pancreatic cancer cells under hypoxia

To evaluate the influence of hypoxia on the expression of BNIP3 in PDAC under hypoxic microenvironment, the CFPAC-1 cells were randomized into four groups and pre-subjected to hypoxia (1% O_2) for 12, 24 or 48 h before the detection of BNIP3 expression with the Western blot assay. Remarkably, hypoxia promoted BNIP3 expression in a time-dependent manner, with the maximum effect achieved by hypoxia for 24 h (Figure 1A and 1B). Meanwhile, the immunofluorescence staining showed a significant increase of BNIP3 expression in CFPAC-1 cells under hypoxia (Figure 1C). Then the CFPAC-1 cells were transfected with BNIP3-specific siRNA (siBNIP3) or a scrambled sequence (siNC). As expected, BNIP3 was significantly downregulated with siBNIP3 transfection (Figure 1D and 1E).

In order to explore the effects of BNIP3 on the migration and proliferation, CFPAC-1 cells transfected with siBNIP3 or siNC were subjected to normoxic or hypoxic condition. Western blot further comfirmed the knockdown of BNIP3 with siRNA transfection (Figure 1F and 1G). As depicted in Figure 1H and 1I, a wound healing assay was performed to evaluate the role of BNIP3 for the cell migration. Results revealed that hypoxia promoted the migration of CFPAC-1 cells, while BNIP3 knockdown suppressed the cell migration under both normoxia and hypoxia condition. In addition, cell motility assay was used to determine the change of single cell motility upon BNIP3 knockdown. Similarily, hypoxia enhanced the motility of CFPAC-1 cells, while BNIP3 knockdown notably downregulated the cell motility under both normoxia and hypoxia condition (Figure 1J and 1K). Moreover, results of the EdU staining and CCK-8 assay revealed that cell proliferation was increased when subjected to hypoxic microenvironment. The inhibition of BNIP3 expression decreased the proliferation of CFPAC-1 cells under both normoxia and hypoxia (Figure 1L, 1M, 1N). These results together indicated that BNIP3 promoted the migration and proliferation of CFPAC-1 cells.

3.2. Autophagy was activated in pancreatic cancer cells under hypoxia

Previously, a great deal of literatures demonstrate that hypoxic microenvironment is an important factor that enhances cell autophagy in solid tumors. Next, we investigated the autophagy flux in CFPAC-1 cells under hypoxia. As shown in Figure 2A and 2B, hypoxia elevated expressions of LC3-II, an important autophagic marker, in a time-dependent manner. To determine whether hypoxia-induced LC3-II requires the transcriptional activity in CFPAC-1 cells, the cells were pretreated with an inhibitor of mRNA synthesis, actinomycin D (ACTD), for 1 h followed by hypoxic treatment for 48 h. ACTD notably suppressed the increase of hypoxia-induced LC3-II and p62 expression (Figure 2C, 2D, 2E), indicating that initial increase in LC3-II and p62 levels depends on the activation of transcriptional machinery under hypoxia. Furthermore, the indirect immunofluorescence staining of endogenous LC3 showed that hypoxia treatment increased the autophagic puncta in CFPAC-1 cells (Figure 2F). Consistently, in LC3-mRFP-GFP adenovirus transfected CFPAC-1 cells, more autolysosomes (red puncta) and autophagosomes (yellow puncta) were found in hypoxia group compared to normoxia group (Figure 2G). Furthermore, to determine whether hypoxia induces autophagic flux, CFPAC-1 cells were treated with a lysosomal inhibitor, chloroquine (CQ), which primarily increases the lysosomal pH, decreases the activity of degradative enzymes and consequently causes the accumulation of vesicular organelles in the cytoplasm, thus inhibiting autophagy. CQ treatment apparently elevated the LC3-II levels in cells under hypoxic conditions compared to normoxic conditions (Figure 2H, 2I, 2J), which indicated the increase in autophagic flux under hypoxia. These observations revealed that autophagy was activated in pancreatic cancer cells under hypoxia.

3.3. BNIP3 involved in the autophagic activation of pancreatic cancer cells under hypoxia

As reported previously, BNIP3 is proved an autophagy regulator in a variety of cancer cells. To explore whether the BNIP3 involves in the activation of autophagy in CFPAC-1 cells under hypoxia, we firstly investigated the interaction of BNIP3 and LC3. Results of immunofluorescence staining demonstrated that the co-localization (yellow dots) of BNIP3 (red dots) and LC3 (green dots) was obviously increased (Figure 3A). Meanwhile, co-immunoprecipitation assay showed a direct interaction of BNIP3 and LC3 in hypoxic CFPAC-1 cells (Figure 3B). Then Western blot was performed to detect the role of BNIP3 for autophagy in CFPAC-1 cells under hypoxia. As depicted in Figure 3C and 3D, BNIP3 knockdown significantly decreased the level of LC3-II, indicating the autophagy inhibition. BafA1 is a specific V-ATPase inhibitor that neutralizes lysosomal pH and block lysosomal degradation. Treating with BafA1 further elevated p62 and LC3-II in CFPAC-1 cells under hypoxia, while BNIP3 knockdown suppressed p62 and LC3-II expression by BafA1 (Figure 3E, 3F, 3G).

Moreover, the indirect immunofluorescence staining of endogenous LC3 demonstrated that knockdown of BNIP3 expression inhibited the formation of hypoxia-induced autophagic puncta in CFPAC-1 cells (Figure 3H). Consistently, in the CFPAC-1 cells transfected with LC3-mRFP-GFP adenovirus, less autophagosomes (yellow puncta) and autolysosomes (red puncta) were found in hypoxia + siBNIP3 group compared to hypoxia + siNC group (Figure 3I). Furthermore, cells were transfected with Ad-GFP-LC3 and Ad-Dsred-Mito to evaluate the mitophagy. The colocalization of LC3 and Mitotracker decreased following BNIP3 knockdown under hypoxia but no change was found under normoxia, which suggested that BNIP3 promoted the mitophagosome formation under hypoxia in CFPAC-1 cells (Figure S1). These results indicated that BNIP3 was responsible for the activation of autophagy and mitophagy in the CFPAC-1 cells under hypoxia.

3.4. Autophagy regulates BNIP3-induced pancreatic cancer cell migration and proliferation under hypoxia

As is well-known that Atg5 involves in the Atg12-Atg5 ubiquitin-like conjugation and direct the elongation and sealing of the autophagosome membrane, Atg7 is an E1-like ligase that conjugates Atg5 to Atg12 [19]. To explore whether autophagy involved in CFPAC-1 cell migration and proliferation under hypoxia treatment, siRNA targeting Atg5 (siAtg5) or Atg7 (siAtg7) was transfected into the cells to suppress autophagy specifically, as confirmed with Western blot (Figure 4A, 4B, 4C, 4B; Figure S2A and S2B). Specific knockdown of Atg5 or Atg7 in CFPAC-1 cells significantly suppressed the LC3-II expression, which revealed the

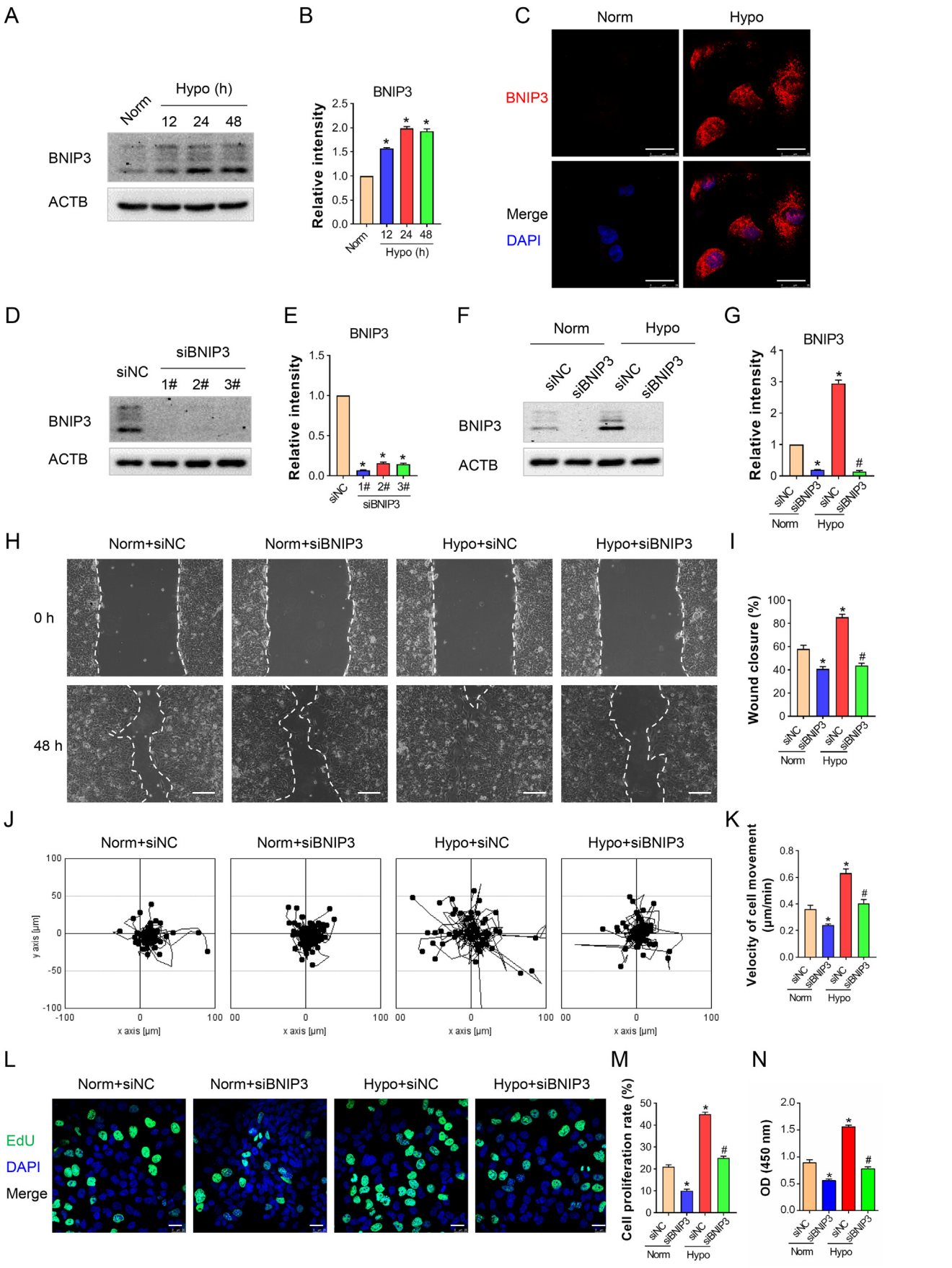

(caption on next page)

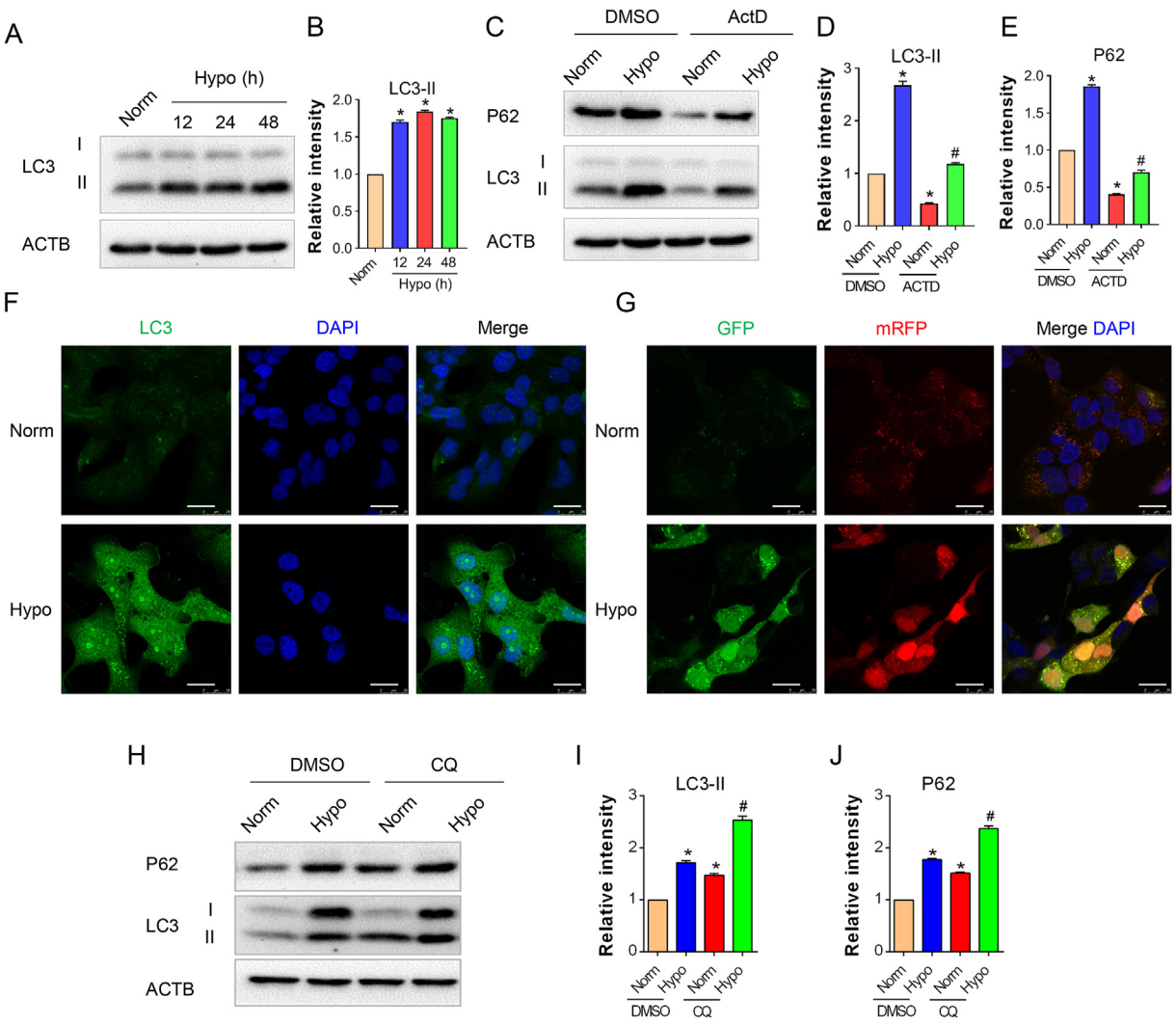

Figure 2. Autophagy was activated in pancreatic cancer cells under hypoxia. CFPAC-1 cells were exposed to hypoxia (1%) and incubated for the indicated times. The protein extracts were analyzed for detection of the autophagy marker LC3-II with Western blot. (A) Representative western blots were shown (n = 3), β-actin was used as a loading control. (B) The graph represents the means ± SEM of the relative integrated signals. *P < 0.05 vs. Norm group. (C) CFPAC-1 cells were treated with actinomycin D (ActD, 5 nM) for 1 h to inhibit transcription. Expressions of P62 and LC3-II were detected using Western blot, β-actin was used as a loading control. (D, E) The graphs represent the means ± SEM of the relative integrated signals. *P < 0.05 vs. Norm + DMSO group, #P < 0.05 vs. Hypo + DMSO group. All the experiments were repeated 3 times. (F) Immunofluorescent staining of LC3 expression (green) was performed in the indicated CFPAC-1 cells (n = 3). Nuclei were stained with DAPI. Scale bar = 25 μm. (G) Representative images of autophagosomes (yellow, GFP^+ $mRFP^+$ puncta) and autolysosomes (red, GFP^- $mRFP^+$ puncta) in Norm and Hypo groups. Nuclei were stained with DAPI (n = 3). Scale bar = 25 μm. (H) CFPAC-1 cells were treated with the lysosomal inhibitor, chloroquine (CQ; 10 μM) before subjected to hypoxia and the autophagy flux was analyzed by Western blot. Representative western blots were shown (n = 3), β-actin was used as a loading control. (I, J) The graph represents the means ± SEM of the relative integrated signals. *P < 0.05 vs. Norm + DMSO group, #P < 0.05 vs. Norm + DMSO group. All the experiments were repeated 3 times.

Figure 1. BNIP3 enhanced the migration and proliferation of pancreatic cancer cells under hypoxia. (A) CFPAC-1 cells were subjected to hypoxia microenvironment for 12, 24 and 48 h and then the BNIP3 expression was detected with Western blot (n = 3), β-actin (ACTB) was used as a loading control. (B) The graph represents the means ± SEM of the relative integrated signals. *P < 0.05 vs. Norm group. (C) Immunofluoresent staining of BNIP3 expression (red) in CFPAC-1 cells subjected to hypoxia for 48 h was shown. Nuclei were stained with DAPI (blue). (D, E) Total protein extracts from cells transfected with BNIP3-specific siRNAs were analyzed using Western blotting to confirm that the siRNA was transfected at comparable levels in CFPAC-1 cells (n = 3). *P < 0.05 vs. siNC group. Then, cells were subjected to hypoxia after transfection with BNIP3 siRNA (siBNIP3) or siRNA-negative control (siNC) for 48 h (F, G), β-actin was used as the loading control (n = 3). (H) Scratch wound healing assays were performed to analyze the migration of indicated cells (n = 3). Images of scratch wounds were captured after 48 h of cultures with or without hypoxia. Scale bar = 200 μm. (I) Graph quantifying the rate of wound closure. The results were presented as the means ± SEM. (J) Single cell motility assays were performed to detect cell motility of indicated groups. Representative images of cell trajectories were shown (n = 3). (K) Graph quantifying the average velocity of cell movement. Results were shown as means ± SEM. (L) After transfection with the indicated siRNAs for 48 h, cell proliferation was evaluated with EdU staining (green) (n = 3). Nuclei were stained with DAPI (blue). (M) Graph quantifying the number of EdU-positive cells in (L). (N) CCK-8 assay was further performed to test the cell proliferation and the results were presented as the means ± SEM. Data are presented as the means ± SEM. *P < 0.05 vs. Norm + siNC group, #P < 0.05 vs. Hypo + siNC group. All the experiments were repeated 3 times. Norm, normoxia; Hypo, hypoxia.

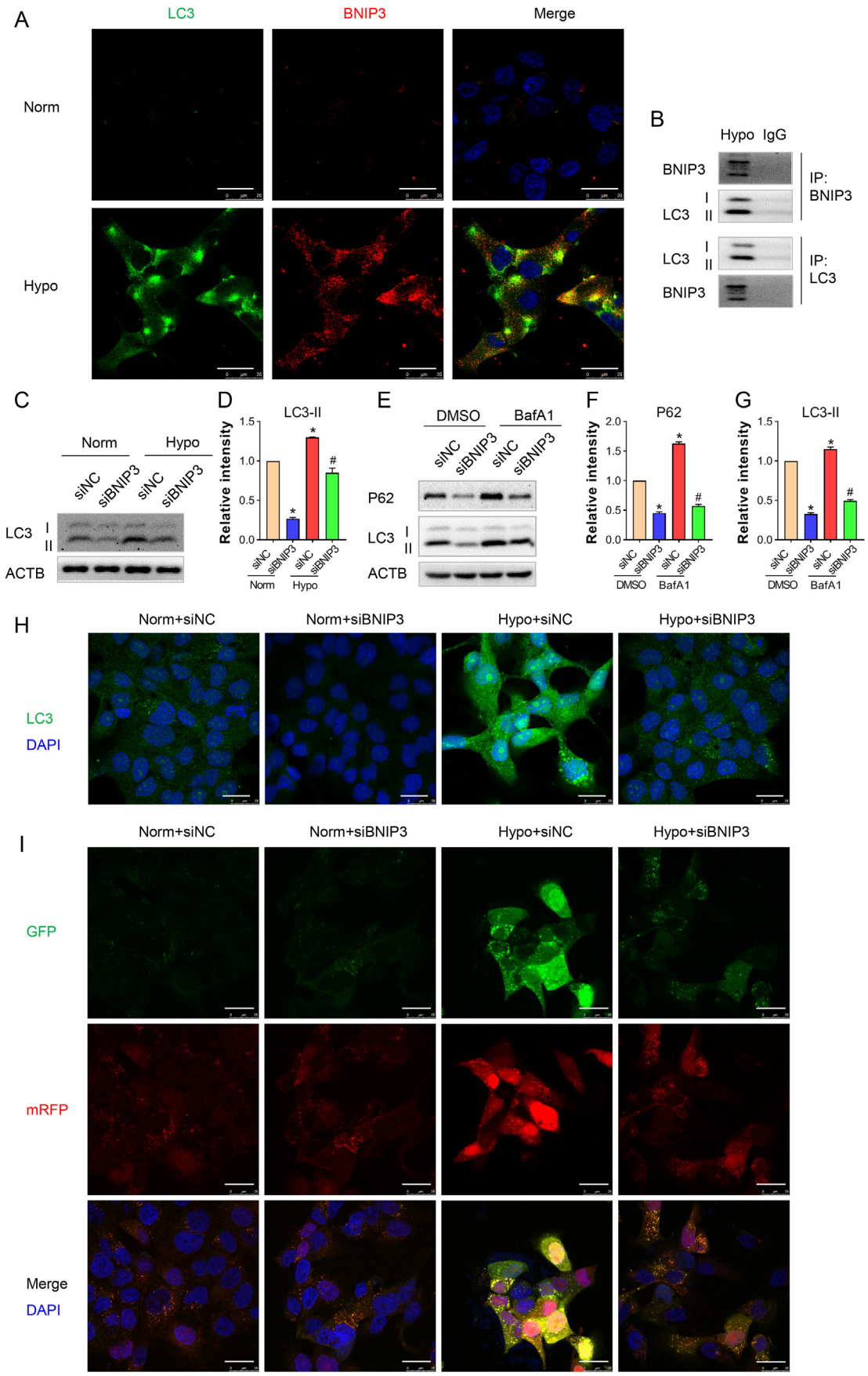

(caption on next page)

inhibition of autophagy (Figure 4C, 4D, 4E; Fig.S2C, S2D, S2E). Meanwhile, Atg5 knockdown obviously inhibited the LC3-II expression by BNIP3 overexpression (Figure S4A).

Basing on the above-mentioned results, we explored if autophagy regulated BNIP3-induced pancreatic cancer cell migration and proliferation under hypoxia. A scratch wound healing assay and a single cell motility assay were respectively performed to investigated cell migration and motility upon the autophagic impairment. Results of the scratch wound model showed that hypoxia significantly promoted the cell migration, while an obvious wound gap remained in the CFPAC-1 cells with Atg5 knockdown (Figure 4F and 4G). As shown in Figure 4H and 4I, knockdown of Atg5 remarkably decreased the range of cell trajectory and the velocity of cell movement, which was in line with the results obtained from the scratch wound healing assay. Moreover, results of EdU staining and CCK-8 assay revealed that the knockdown of Atg5 expression decreased the proliferation of CFPAC-1 cells under both normoxia and hypoxia (Figure 1J, 1K, 1L). Similar results were found in CFPAC-1 cells with Atg7 knockdown (Figure S2F, S2G, S2H, S2I, S2J, S2K, S2L). Furthermore, Atg5-targeting siRNA was transfected in CFPAC-1 cells with BNIP3 overexpression to inhibit autophagy. As shown in Figure S4B and S4C, Atg5 knockdown resulted in a larger wound gap, a smaller range of cell trajectory and a lower speed of cell movement compared with the BNIP3-overexpressed group. Results of the EdU staining and CCK-8 assay demonstrated a significant reduction of cell proliferation upon Atg5 knockdown in BNIP3-overexpressed group (Figure S4D and S4E). Together, these results suggust that autophagy involves in the BNIP3-induced pancreatic cancer cell migration and proliferation under hypoxia.

3.5. ERK1/2 signaling pathway involves in the regulation of BNIP3-autophagy axis under hypoxia

To gain further insights into the mechanisms responsible for the activation of BNIP3-autophagy in the hypoxia-induced CFPAC-1 cell migration under hypoxia treatment, we first investigated the activation of ERK1/2 signaling pathway. CFPAC-1 cells were randomized into four groups and pre-subjected to hypoxia (1% O_2) for 12, 24 or 48 h before the detection of ERK1/2 activation with the Western blot assay. Notably, hypoxia enhanced the ERK1/2 activation in a time-dependent manner, and achieved the maximum effect by hypoxia for 24 h (Figure 5A and 5B). Then a selective chemical inhibitor was used to suppress the activation of ERK1/2 signaling. The addition of PD98058 decreased the expressions of BNIP3 and LC3-II under normoxia condition (Figure S3A and S3B), and it was significant that hypoxia-induced elevation of BNIP3 and LC3-II were both ameliorated by the inhibition of ERK1/2 signaling as shown by Western blot (Figure 5C and 5D), which was also confirmed with the immunofluorescence staining under confocal microscope (Figure 5E, 5F, 5G). Moreover, the overexpression of BNIP3 by lentivirus infection could reversed the downregulation of LC3-II by the inhibition of ERK1/2 pathway (Figure S5A). These results suggested that ERK1/2 signaling pathway participate in the activation of BNIP3-autophagy axis in CFPAC-1 cells under hypoxia.

Next, the EdU staining and CCK-8 assay were used to evaluate the proliferation of indicated CFPAC-1 cells. As shown in Figure 5H and 5I and Figure S3C-S3E, inhibition of ERK1/2 induced a remarkable decrease in the proliferation of CFPAC-1 cells under normoxia and hypoxia. The single cell motility assay showed that inhibition of ERK1/2 significant attenuated the cell motility, as represented by the inhibition in the range of cell trajectory and the velocity of cell movement (Figure 5J and 5K and Figure S3F and S3G). Consistently, results of the scratch wound healing assay demonstrated an obvious wound gap remained in the CFPAC-1 cells with ERK1/2 inhibition (Figure 5L and 5M and Figure S3H and S3I). Furthermore, BNIP3 overexpression reversed the impairment of cell migration and proliferation by ERK1/2 inhibition (Figure S5B, S5C, S5D, S5E). Taken with the results above, inhibition of ERK1/2 signaling attenuated the elevation of BNIP3 expression, as well as the activation of autophagy, and consequently suppressed the proliferation and migration of CFPAC-1 cells under hypoxia.

3.6. BNIP3 enhanced the migration and proliferation of Panc1 cells under hypoxia

In order to test whether BNIP3 generally promotes the migration and proliferation of pancreatic cancer cells, we test its role in Panc1 cells under hypoxia. The Panc1 cells were transfected with lentivirus or siRNA for the overexpression or knockdown of BNIP3. As expected, BNIP3 in Panc1 cells was significantly overexpressed by AdBNIP3 infection and downregulated with siBNIP3 transfection, respectively. The upregulation of BNIP3 induced the increase of LC3-II, while the knockdown of BNIP3 impaired the elevation of LC3-II under hypoxia (Figure 6A), which suggested a similar decrease of autophagy under hypoxia as in the CFPAC-1 cells. Then, a wound healing assay (Figure 6B) and a cell motility assay (Figure 6C) were used to evaluate the effects of BNIP3 on the migration of Panc1 cells. Results demonstrated that BNIP3 overexpression promoted the cell migration, hypoxia promoted the migration and of Panc1 cells, while BNIP3 knockdown suppressed the cell migration under hypoxia. Moreover, results of EdU staining and CCK-8 assay revealed that BNIP3 overexpression increased the cell proliferation under normoxia, inhibition of BNIP3 expression decreased the proliferation of Panc1 cells under hypoxia (Figure 6D, 6E, 6F). These results indicated that BNIP3 promoted the migration and proliferation of Panc1 cells.

In order to evaluate the involvement of autophagy in BNIP3-induced migration and proliferation of Panc1 cells, Atg5-siRNA was transfected in the BNIP3-overexpressed Panc1 cells. Western blot showed a significant downregulation of the BNIP3-induced LC3-II expression with the knockdown of Atg5 (Figure 6G). Results of the wound healing assay (Figure 6H and 6I) and cell motility assay (Figure 6J) showed a significant inhibition of the BNIP3-induced migration. Next, the EdU staining and CCK-8 assay was applied to investigate the proliferation of indicated Panc1 cells. As shown in Figure 6K, 6L, 6M, the BNIP3-induced proliferation of Panc1 cells was attenuated by the knockdown of Atg5. These results indicated that autophagy acted a role in the BNIP3-induced migration and proliferation of Panc1 cells under hypoxia.

Then, the role of ERK1/2 pathway in BNIP3/autophagy-regulated migration and proliferation of Panc1 cells was investigated. As depicted in Figure 6N, inhibition of ERK1/2 pathway obviously suppressed the expressions of BNIP3 and LC3-II under hypoxia, while the overexpression of BNIP3 by lentivirus infection could reversed the downregulation of

Figure 3. BNIP3 was involved in the activation of autophagy in pancreatic cancer cells under hypoxia. CFPAC-1 cells were exposed to hypoxia (1%) and incubated for the 48 h. (A) Costaining of BNIP3 (red) and LC3 (green) in CFPAC-1 cells was performed with corresponding antibodies and visualized via confocal microscopy. Nuclei were stained with DAPI (blue). Scale bar = 25 μm. (B) The CFPAC-1 cells under hypoxia were lysed and immunoprecipitated with anti-BNIP3 or anti-LC3 antibody followed by immunoblotting with anti-LC3 or anti-BNIP3 antibody. (C) LC3 expression in the BNIP3-siRNA transfected cells under normoxia or hypoxia were determined using Western blotting. β-Actin was used as the loading control (n = 3). (D) The graph represents the means ± SEM of the relative integrated signals. *P < 0.05 vs. Norm + siNC group, #P < 0.05 vs. Hypo + siNC group. (E) Autophagy inhibitors, Bafilomycin A1 (BafA1, 10 nM) was added 1 h prior to hypoxia exposure. The extracted proteins were immunoblotted with the indicated antibodies. β-Actin was used as the loading control (n = 3). (F, G) The graphs represented the means ± SEM of the relative integrated signals. *P < 0.05 vs. DMSO + siNC group, #P < 0.05 vs. BafA1+siNC group. (H) Immunofluorescent staining of LC3 expression (green) with an antibody was performed in the indicated CFPAC-1 cells (n = 3). Nuclei were stained with DAPI. Scale bar = 25 μm. (I) Representative images of autophagosomes (yellow, GFP^+ $mRFP^+$ puncta) and autolysosomes (red, GFP^- $mRFP^+$ puncta) in Norm and Hypo groups. Nuclei were stained with DAPI (n = 3). Scale bar = 25 μm. All the experiments were repeated 3 times.

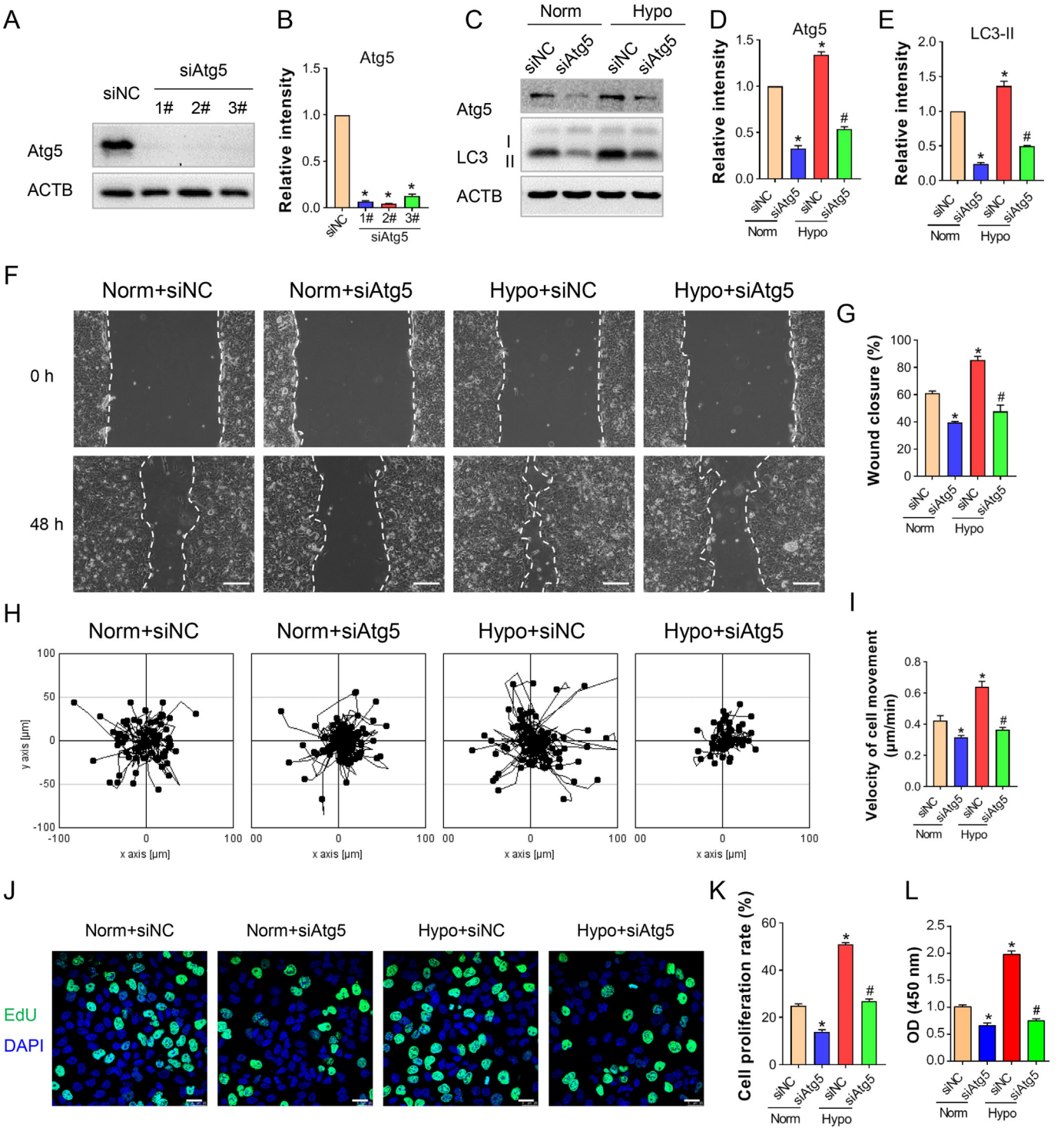

Figure 4. Autophagy regulates pancreatic cancer cell migration and proliferation under hypoxia. To elucidate whether autophagy was involved in CFPAC-1 cell migration and proliferation under hypoxia, siRNA targeting Atg5 (siAtg5) was applied for the knockdown of Atg5. (A) Western blot was performed to analyze the effects of siRNA on the expression of Atg5 (n = 3). Representative bands were shown, β-actin was used as the loading control. (B) The graph represents the means ± SEM of the relative integrated signals. *P < 0.05 vs. siNC group. (C) The effects of Atg5 knockdown by siRNA on autophagy was evaluated (n = 3), and representative bands were shown. (D, E) The graph represents the means ± SEM of the relative integrated signals. (F) Scratch wound healing assays were used for detection of the migration of indicated cells (n = 3). Representative images of scratched wound were shown. Scale bar = 200 μm. (G) Graph quantifying the rate of wound closure. Results were shown as means ± SEM. (H) Single cell motility assays were performed to detect the motility of indicated CFPAC-1 cells (n = 3). Representative images of cell trajectories were shown. (I) Graph quantifying the average velocity of cell movement. Results were shown as means ± SEM. (J) After transfection with the indicated siRNAs for 48 h, cell proliferation was determined with EdU staining (green) (n = 3). Nuclei were stained with DAPI (blue). (K) Graph quantifying the number of EdU-positive cells. Data are presented as the means ± SEM. (L) CCK-8 assay was further performed to test the cell proliferation and the results were presented as the means ± SEM. *P < 0.05 vs. Norm + siNC group, #P < 0.05 vs. Hypo + siNC group. All the experiments were repeated 3 times.

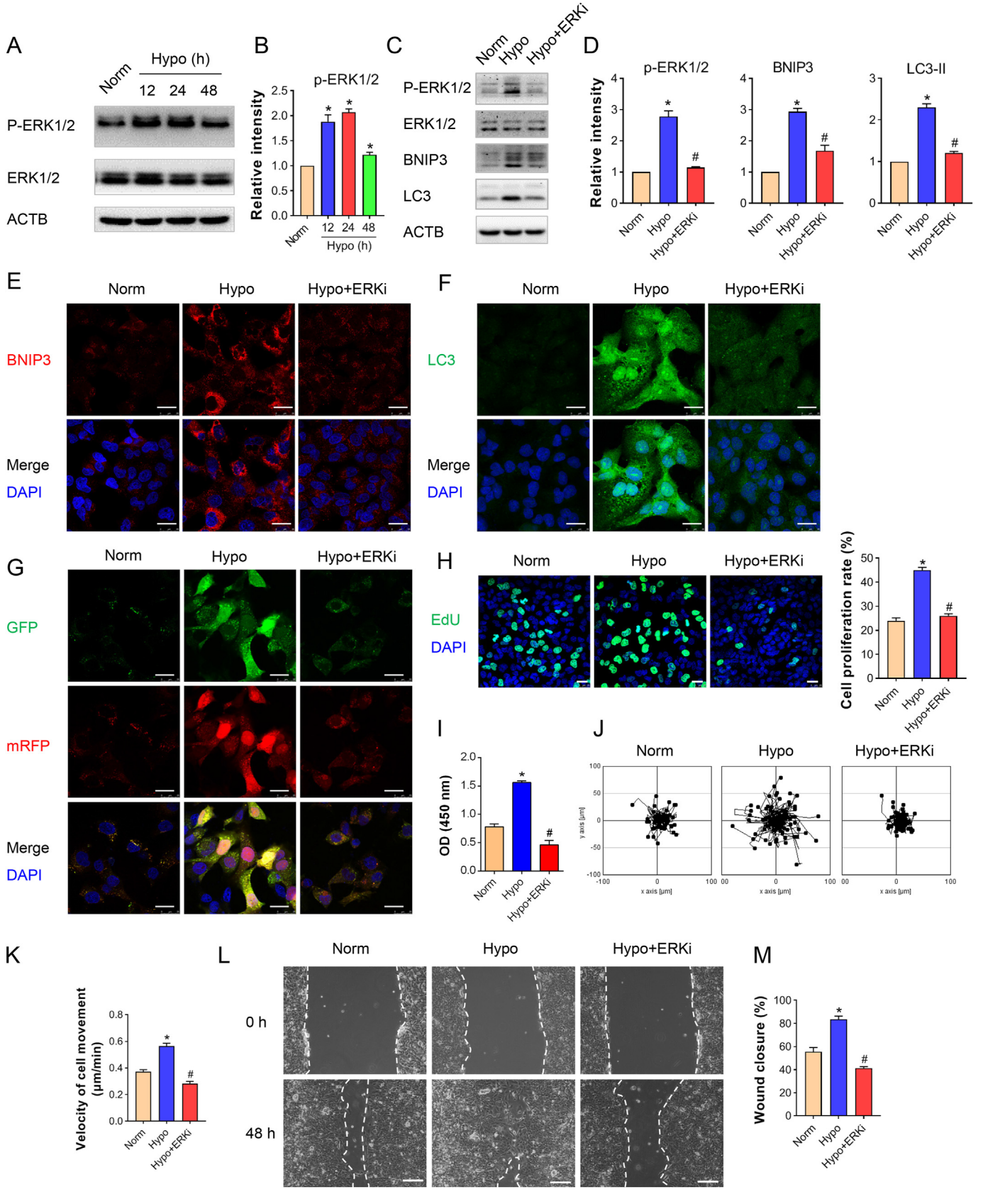

(caption on next page)

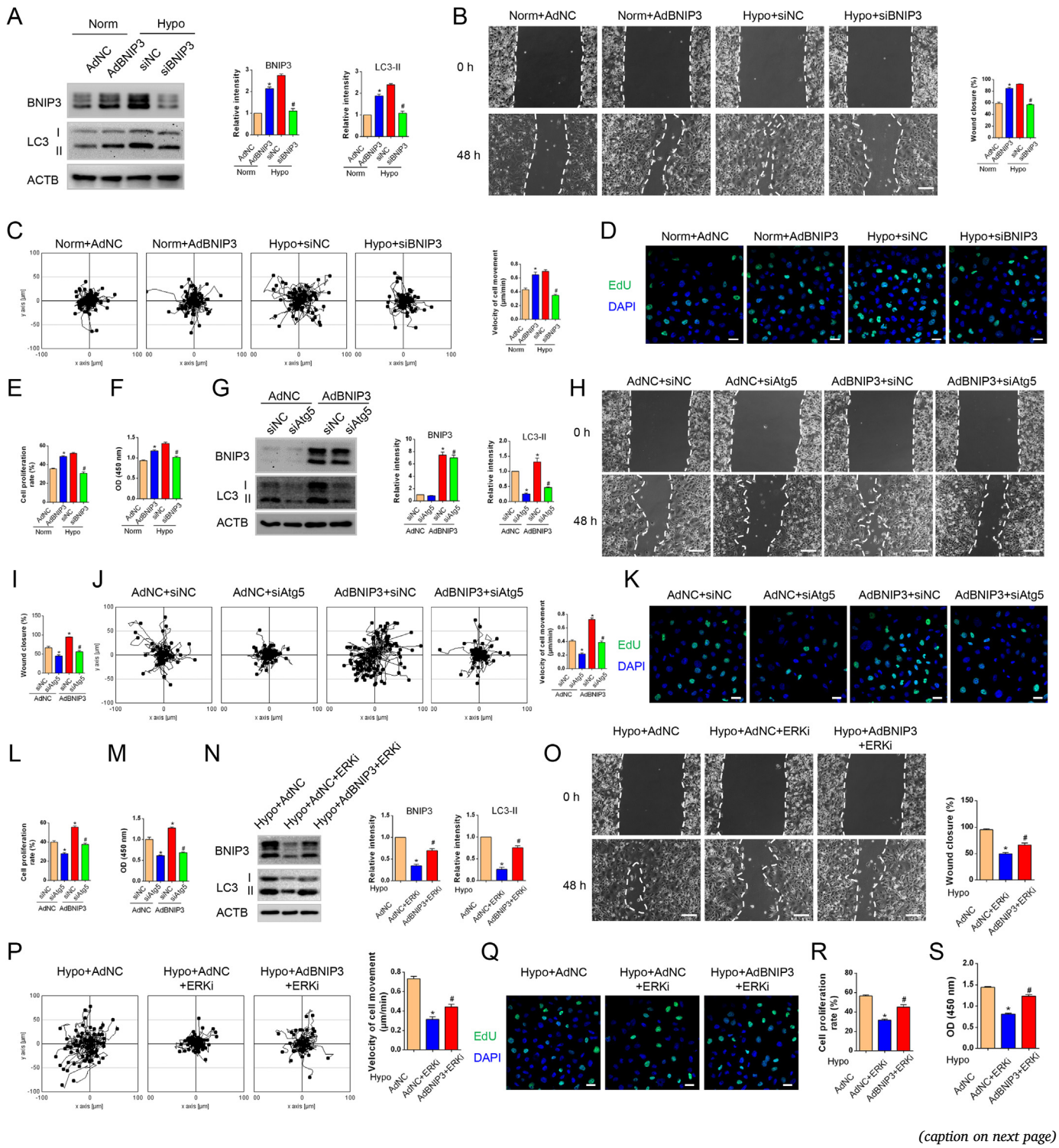

(caption on next page)

Figure 5. ERK1/2 signaling pathway involves in the regulation of BNIP3-autophagy axis under hypoxia. CFPAC-1 cells were subjected to hypoxia for 12, 24 and 48 h and then ERK1/2 activity was detected with Western blot (n = 3). β-Actin was used as a loading control. (B) The graph represents the means ± SEM of the relative integrated signals. (C) As a specific inhibitor of ERK1/2 signaling, PD98058 (work concentration: 10 μM) was used to suppress the activation of ERK1/2 signaling. Western blot was performed to detect the expressions of LC3-II and BNIP3 upon ERK1/2 inhibition in CFPAC-1 cells under hypoxia. (D) The graph represents the means ± SEM of the relative integrated signals. (E, F) Fluorescence staining of BNIP3 (red) and LC3 (green) was performed in the indicated CFPAC-1 cells (n = 3). Nuclei were stained with DAPI. Scale bar = 25 μm. (G) Representative images of autophagosomes (yellow, GFP^+ $mRFP^+$ puncta) and autolysosomes (red, GFP^- $mRFP^+$ puncta) in the indicated groups. Nuclei were stained with DAPI (n = 3). Scale bar = 25 μm. (H) Effects of ERK1/2 inhibition on cell proliferation was determined with EdU staining (green) (n = 3). Nuclei were stained with DAPI (blue). Graph quantifying the number of EdU-positive cells was shown in the right pannel. (I) CCK-8 assay was further performed to test the cell proliferation and the results were presented as the means ± SEM. (J) Single cell motility assays were performed to detect the motility of indicated CFPAC-1 (n = 3). (K) Graph quantifying the average velocity of cell movement. Results were shown as means ± SEM, as shown in the right pannel. (L) Scratch wound healing assays were performed to detect the migration of indicated cells (n = 3). Representative pictures of the scratched wound were shown. Scale bar = 100 μm. (M) Graph quantifying the rate of wound closure was demonstrated as means ± SEM. *P < 0.05 vs. Norm group, #P < 0.05 vs. Hypo group. All the experiments were repeated 3 times.

LC3-II by the inhibition of ERK1/2 pathway. Results of the wound healing assay (Figure 6O) demonstrated an obvious wound gap remained in the Panc1 cells with ERK1/2 inhibition under hypoxia, BNIP3 overexpression significantly promoted the healing of the "scratched wound". Similarly, the single cell motility assay showed that inhibition of ERK1/2 significant decreased the range of cell trajectory and the velocity of cell movement (Figure 6P). Furthermore, the EdU staining and CCK-8 assay were applied to investigate the cell proliferation. As shown in Figure 6Q, 6R, 6S, inhibition of ERK1/2 induced a remarkable decrease in the proliferation of Panc1 cells under hypoxia, which could be promoted by the BNIP3 overexpression. Taken together, these results revealed that the ERK1/2 signaling elevated the BNIP3 expression and activated autophagy, which consequently promoted the proliferation and migration of Panc1 cells under hypoxia.

4. Discussion

Pancreatic ductal adenocarcinoma (PDAC) is one of the most deadly cancers, while little advances in treatment are reported in the past decades. PDAC contains abundant stromal cells, lacks vascularization, thus persistent hypoxia is accompanied within the tumors [1]. It has been reported that hypoxic microenvironment induces the aggressive characteristics of cancer cells in many types of cancer, including pancreatic cancer, while the potential molecular mechanisms need further studies in-depth.

BNIP3 is a hypoxia-responsive protein and plays an important role in the progress and metastasis of multiple cancers. As a pro-apoptotic atypical BH3-only protein, BNIP3 involves in cell necrosis, apoptosis, or autophagy depending on the cellular context. Recently, BNIP3 has been demonstrated to promote keratinocyte migration in an autophagy-dependent way [20]. Consistently, the results here showed that the expressions of BNIP3 and the hallmarks of autophagy were remarkably increased in CFPAC-1 and Panc1 cells under hypoxia, accompanied with the elevations of cell migration and proliferation, as determined respectively with the scratched wound-healing assay, single-cell motility assay, EdU staining and CCK-8 assay. Knockdown of BNIP3 with siRNA transfection significantly impaired the proliferation and migration of CFPAC-1 cells, as well as the autophagy flux as determined with Western blot and immunofluoresent staining. Moreover, the interaction of BNIP3 and LC3-II was revealed with CO-IP and co-localization assay. Furthermore, the hypoxia-induced CFPAC-1 migration and proliferation was notably suppressed by the inhibition of autophagy with the Atg5-or Atg7-targeted siRNAs. Meanwhile, the overexpression of BNIP3 by the lentivirus infection enhanced the migration and proliferation of CFPAC-1 and Panc1 cells, which could be disturbed by Atg5 knockdown. These results together indicated that BNIP3-mediated autophagy promoted the migration and proliferation of pancreatic cancer cells.

BNIP3 expression is usually transcriptionally regulated by hypoxia-inducible factor 1α (HIF-1α), a major transcription factor in hypoxia [7]. To date, studies have revealed several HIF-1α−independent mechanisms that mediate BNIP3 expression. For example, BNIP3 expression under energy stress and in pathological cardiac hypertrophy is modulated by forkhead box (FOX)O transcription factor [21, 22]; Sp3 might be the major transcriptional regulator of BNIP3 in prostate cancer [23]. The mitogen-activated protein kinase (MAPK) cascades transduce the signaling of stress-induced stimuli or extracellular growth factor, and play crucial roles for the control of cell migration, proliferation, and survival [24, 25]. In hepatocellular carcinoma, phosphorylation of JNK closely binds to the promoter of *BNIP3* gene and contributes to BNIP3 expression [26]. As recently reported, BNIP3 expression was upregulated by P38 and JNK signaling in keratinocytes under hypoxia [20]. In this study, we reported that extracellular-signal-regulated kinase (ERK) played a role in the upregulation of BNIP3 expression in hypoxic pancreatic cancer cells. Maybe hypoxia-induced ERK phosphorylation can also bind to the promoter of *BNIP3* gene and regulate its expression, which remains further investigations.

Autophagy is a conserved process in eukaryotic cells that recycles the altered or unused organelles and cellular components and delivers them to the lysosome for degradation. Autophagy has been reported to involve in migration and growth of both normal and cancerous cells, while the molecular mechanisms remains largely unknown. Previously, autophagy has been shown to regulate recycling of β1 integrin membranes, depolymerization of focal adhesions, and acquisition of mesenchymal markers, which are essential for cell migration [27, 28, 29, 30, 31]. Mitochondria are potential targets for hypoxia-induced autophagy. The mitochondria dynamics provide energy supplement for the reorganization of cytoskeleton and sustaining the cell migration [32]. Autophagy has been shown to be upregulated in PDAC and involved in resistance to cytotoxic chemotherapy and targeted therapy, while the molecular mechanisms that activate autophagy in PDAC have only just begun to

Figure 6. BNIP3 enhanced the migration and proliferation of Panc1 cells under hypoxia. (A) Panc1 cells were infected with AdBNIP3 or transfected with siBNIP3 for the interfering of BNIP3 expression, then Western blot was performed (n = 3), β-actin (ACTB) was used as a loading control. The graph represents the means ± SEM of the relative integrated signals. *P < 0.05 vs. Norm + AdNC group, #P < 0.05 vs. Hypo + siNC group. (B) Scratch wound healing assays were performed to analyze the migration of indicated cells (n = 3). Images of scratch wounds were captured after 48 h of cultures with or without hypoxia. Scale bar = 200 μm. Graph quantifying the rate of wound closure. The results were presented as the means ± SEM. *P < 0.05 vs. Norm + AdNC group, #P < 0.05 vs. Hypo + siNC group. (C) Single cell motility assays were performed to detect cell motility of indicated groups. Representative images of cell trajectories were shown (n = 3). Graph quantifying the average velocity of cell movement. Results were shown as means ± SEM. *P < 0.05 vs. Norm + AdNC group, #P < 0.05 vs. Hypo + siNC group. (D) Cell proliferation was evaluated with EdU staining (green) (n = 3). Nuclei were stained with DAPI (blue). (E) Graph quantifying the number of EdU-positive cells in (D). (F) CCK-8 assay was further performed to test the cell proliferation and the results were presented as the means ± SEM. Data are presented as the means ± SEM. *P < 0.05 vs. Norm + AdNC group, #P < 0.05 vs. Hypo + siNC group. (G) siAtg5 or siNC was transfected in Panc1 cells with BNIP3 overexpression, and Western blot was performed to analyze the expression of BNIP3 and LC3-II. Results were shown as means ± SEM. *P < 0.05 vs. AdNC + siNC group, #P < 0.05 vs. AdBNIP3+siNC group. (H) Scratch wound healing assays were performed to analyze the migration of indicated cells (n = 3). Images of scratch wounds were captured after 48 h of cultures. Scale bar = 200 μm. (I) Graph quantifying the rate of wound closure. The results were presented as the means ± SEM. *P < 0.05 vs. *P < 0.05 vs. AdNC + siNC group, #P < 0.05 vs. AdBNIP3+siNC group. (J) Single cell motility assays were performed to detect cell motility of indicated groups. Representative images of cell trajectories were shown (n = 3). Graph quantifying the average velocity of cell movement. Results were shown as means ± SEM. *P < 0.05 vs. *P < 0.05 vs. AdNC + siNC group, #P < 0.05 vs. AdBNIP3+siNC group. (K) Cell proliferation was evaluated with EdU staining (green) (n = 3). Nuclei were stained with DAPI (blue). (L) Graph quantifying the number of EdU-positive cells in (K). (M) CCK-8 assay was further performed to test the cell proliferation and the results were presented as the means ± SEM. (N) Western blot was performed to detect the expressions of LC3-II and BNIP3 upon ERK1/2 inhibition in Panc1 cells with BNIP3 overexpression under hypoxia. The graph represents the means ± SEM of the relative integrated signals. *P < 0.05 vs. Hypo + AdNC group, #P < 0.05 vs. Hypo + AdNC + ERKi group. (O) Scratch wound healing assays were performed to analyze the migration of indicated cells (n = 3). Images of scratch wounds were captured after 48 h of cultures. Scale bar = 200 μm. Graph quantifying the rate of wound closure. The results were presented as the means ± SEM. *P < 0.05 vs. Hypo + AdNC group, #P < 0.05 vs. Hypo + AdNC + ERKi group. (P) Single cell motility assays were performed to detect cell motility of indicated groups. Representative images of cell trajectories were shown (n = 3). Graph quantifying the average velocity of cell movement. Results were shown as means ± SEM. *P < 0.05 vs. Hypo + AdNC group, #P < 0.05 vs. Hypo + AdNC + ERKi group. (Q) Cell proliferation was evaluated with EdU staining (green) (n = 3). Nuclei were stained with DAPI (blue). (R) Graph quantifying the number of EdU-positive cells in (Q). (S) CCK-8 assay was further performed to test the cell proliferation and the results were presented as the means ± SEM. *P < 0.05 vs. Hypo + AdNC group, #P < 0.05 vs. Hypo + AdNC + ERKi group. All the experiments were repeated 3 times. Norm, normoxia; Hypo, hypoxia.

emerge. Recently, Wong et al. showed that phosphatase PP2A increased the activity of UNC-51-like kinase 1 (ULK1) and participated in the initiation of autophagy, which was also responsible for increased autophagy in PDAC cells [33]. In addition, Settembre et al. reported that the starvation-induced TFEB nuclear translocation in HeLa cells was suppressed by ERK/MAPK2-mediated phosphorylation [34], which was also observed in PDAC models that inhibition of RAS–RAF–MEK–ERK/MAPK signaling pathway resulted in increased autophagic flux [35, 36]. These results indicate that ERK/MAPK signaling is clearly involved in autophagy regulation of PDAC. Here, our results demonstrated a BNIP3-dependent way of autophagy activation in CFPAC-1 and Panc1 cells under hypoxia. The ERK/MAPK signaling pathway was obviously upregulated under hypoxia, and the elevations of BNIP3 expression and activation of autophagy was both suppressed by the ERK/MAPK inhibitor, which consequently inhibited the cell migration and proliferation. Moreover, BNIP3 overexpression significantly reversed the impairment of cell migration and proliferation, as well as the activation of autophagy, by ERK1/2 inhibition. The above observations indicate that autophagy is a therapeutic target for PDAC, and the combination of ERK/MAPK pathway inhibitors and autophagy inhibitors may be an effective treatment for PDAC.

Together, our current work demonstrated that BNIP3-induced autophagy was involved in the migration and proliferation of PDAC cells under hypoxia. Meanwhile, ERK/MAPK signaling is significant activated and enhances BNIP3-mediated autophagy in CFPAC-1 cells under hypoxia, and consequently promotes PDAC cell migration and proliferation. These results reveal a new molecular explanation for the autophagy activation in PDAC.

Declarations

Author contribution statement

Xiaojiao Wang: Conceived and designed the experiments; Contributed reagents, materials, analysis tools or data; Analyzed and interpreted the data; Wrote the paper.

Hongmei Li; Can Zhang: Conceived and designed the experiments; Performed the experiments; Analyzed and interpreted the data; Wrote the paper.

Qiong Zhang; Jiezhi Jia: Performed the experiments; Analyzed and interpreted the data.

Funding statement

Xiaojiao Wang was supported by National Natural Science Foundation of China [82103441].

Data availability statement

The data that has been used is confidential.

Declaration of interest's statement

The authors declare no conflict of interest.

Additional information

Supplementary content related to this article has been published online at https://doi.org/10.1016/j.heliyon.2022.e11190.

References

[1] A.A. Connor, S. Gallinger, Pancreatic cancer evolution and heterogeneity: integrating omics and clinical data, Nat. Rev. Cancer (2021).
[2] W. Lin, P. Noel, E.H. Borazanci, J. Lee, A. Amini, I.W. Han, J.S. Heo, G.S. Jameson, C. Fraser, M. Steinbach, et al., Single-cell transcriptome analysis of tumor and stromal compartments of pancreatic ductal adenocarcinoma primary tumors and metastatic lesions, Genome Med. 12 (1) (2020) 80.
[3] K. Yamamoto, A. Venida, J. Yano, D.E. Biancur, M. Kakiuchi, S. Gupta, A.S.W. Sohn, S. Mukhopadhyay, E.Y. Lin, S.J. Parker, et al., Autophagy promotes immune evasion of pancreatic cancer by degrading MHC-I, Nature 581 (7806) (2020) 100–105.
[4] K. Koikawa, S. Kibe, F. Suizu, N. Sekino, N. Kim, T.D. Manz, B.J. Pinch, D. Akshinthala, A. Verma, G. Gaglia, et al., Targeting Pin1 renders pancreatic cancer eradicable by synergizing with immunochemotherapy, Cell 184 (18) (2021).
[5] A. Yamasaki, K. Yanai, H. Onishi, Hypoxia and pancreatic ductal adenocarcinoma, Cancer Lett. (2020) 484.
[6] P.C. McDonald, S.C. Chafe, W.S. Brown, S. Saberi, M. Swayampakula, G. Venkateswaran, O. Nemirovsky, J.A. Gillespie, J.M. Karasinska, S.E. Kalloger, et al., Regulation of pH by carbonic anhydrase 9 mediates survival of pancreatic cancer cells with activated KRAS in response to hypoxia, Gastroenterology 157 (3) (2019) 823–837.
[7] J. Zhang, P.A. Ney, Role of BNIP3 and NIX in cell death, autophagy, and mitophagy, Cell Death Differ. 16 (7) (2009) 939–946.
[8] Z.-J. Fu, Z.-Y. Wang, L. Xu, X.-H. Chen, X.-X. Li, W.-T. Liao, H.-K. Ma, M.-D. Jiang, T.-T. Xu, J. Xu, et al., HIF-1α-BNIP3-mediated mitophagy in tubular cells protects against renal ischemia/reperfusion injury, Redox Biol. 36 (2020), 101671.
[9] A.S. Gorbunova, M.A. Yapryntseva, T.V. Denisenko, B. Zhivotovsky, BNIP3 in lung cancer: to kill or rescue? Cancers 12 (11) (2020).
[10] Y. Qu, S. Dang, P. Hou, Gene methylation in gastric cancer, Clin. Chim. Acta 424 (2013) 53–65.
[11] A.H. Chourasia, K.F. Macleod, Tumor suppressor functions of BNIP3 and mitophagy, Autophagy 11 (10) (2015) 1937–1938.
[12] D.P. Panigrahi, P.P. Praharaj, C.S. Bhol, K.K. Mahapatra, S. Patra, B.P. Behera, S.R. Mishra, S.K. Bhutia, The emerging, multifaceted role of mitophagy in cancer and cancer therapeutics, Semin. Cancer Biol. 66 (2020) 45–58.
[13] T. Yamazaki, J.M. Bravo-San Pedro, L. Galluzzi, G. Kroemer, F. Pietrocola, Autophagy in the cancer-immunity dialogue, Adv. Drug Deliv. Rev. 169 (2021) 40–50.
[14] H. Folkerts, S. Hilgendorf, E. Vellenga, E. Bremer, V.R. Wiersma, The multifaceted role of autophagy in cancer and the microenvironment, Med. Res. Rev. 39 (2) (2019) 517–560.
[15] M. Piffoux, E. Eriau, P.A. Cassier, Autophagy as a therapeutic target in pancreatic cancer, Br. J. Cancer 124 (2) (2021) 333–344.
[16] H. Su, F. Yang, R. Fu, X. Li, R. French, E. Mose, X. Pu, B. Trinh, A. Kumar, J. Liu, et al., Cancer cells escape autophagy inhibition via NRF2-induced macropinocytosis 39, 2021, pp. 678–693, e611.
[17] C. Stalnecker, K. Grover, A. Edwards, M. Coleman, R. Yang, J. DeLiberty, B. Papke, C. Goodwin, M. Pierobon, E. Petricoin, et al., Concurrent Inhibition of IGF1R and ERK Increases Pancreatic Cancer Sensitivity to Autophagy Inhibitors, 2021.
[18] A. Salic, T.J. Mitchison, A chemical method for fast and sensitive detection of DNA synthesis in vivo, Proc. Natl. Acad. Sci. U. S. A 105 (7) (2008) 2415–2420.
[19] J.J. Collier, F. Suomi, M. Oláhová, T.G. McWilliams, R.W. Taylor, Emerging roles of ATG7 in human health and disease, EMBO Mol. Med. 13 (12) (2021), e14824.
[20] J. Zhang, C. Zhang, X. Jiang, L. Li, D. Zhang, D. Tang, T. Yan, Q. Zhang, H. Yuan, J. Jia, et al., Involvement of autophagy in hypoxia-BNIP3 signaling to promote epidermal keratinocyte migration, Cell Death Dis. 10 (3) (2019) 234.
[21] A. Lin, J. Yao, L. Zhuang, D. Wang, J. Han, E.W. Lam, T.R. Network, B. Gan, The FoxO-BNIP3 axis exerts a unique regulation of mTORC1 and cell survival under energy stress, Oncogene 33 (24) (2014) 3183–3194.
[22] A.H. Chaanine, D. Jeong, L. Liang, E.R. Chemaly, K. Fish, R.E. Gordon, R.J. Hajjar, JNK modulates FOXO3a for the expression of the mitochondrial death and mitophagy marker BNIP3 in pathological hypertrophy and in heart failure, Cell Death Dis. 3 (2012) 265.
[23] Y. Huang, P. Shen, X. Chen, Z. Chen, T. Zhao, N. Chen, J. Gong, L. Nie, M. Xu, X. Li, et al., Transcriptional regulation of BNIP3 by Sp3 in prostate cancer, Prostate 75 (14) (2015) 1556–1567.
[24] C. Anerillas, K. Abdelmohsen, M. Gorospe, Regulation of senescence traits by MAPKs, GeroScience 42 (2) (2020) 397–408.
[25] S. Papa, P. Choy, C.J.O. Bubici, The ERK and JNK pathways in the regulation of metabolic reprogramming 38, 2019, pp. 2223–2240.
[26] C. Shi, Y. Cai, Y. Li, Y. Li, N. Hu, S. Ma, S. Hu, P. Zhu, W. Wang, H. Zhou, Yap promotes hepatocellular carcinoma metastasis and mobilization via governing cofilin/F-actin/lamellipodium axis by regulation of JNK/Bnip3/SERCA/CaMKII pathways, Redox Biol. 14 (2018) 59–71.
[27] T. Sun, L. Jiao, Y. Wang, Y. Yu, L. Ming, SIRT1 induces epithelial-mesenchymal transition by promoting autophagic degradation of E-cadherin in melanoma cells, Cell Death Dis. 9 (2) (2018) 136.
[28] H. Liu, Y. Ma, H.W. He, W.L. Zhao, R.G. Shao, SPHK1 (sphingosine kinase 1) induces epithelial-mesenchymal transition by promoting the autophagy-linked lysosomal degradation of CDH1/E-cadherin in hepatoma cells, Autophagy 13 (5) (2017) 900–913.
[29] M.N. Sharifi, E.E. Mowers, L.E. Drake, C. Collier, H. Chen, M. Zamora, S. Mui, K.F. Macleod, Autophagy promotes focal adhesion disassembly and cell motility of metastatic tumor cells through the direct interaction of paxillin with LC3, Cell Rep. 15 (8) (2016) 1660–1672.
[30] C.M. Kenific, T. Wittmann, J. Debnath, Autophagy in adhesion and migration, J. Cell Sci. 129 (20) (2016) 3685–3693.
[31] V. Tuloup-Minguez, A. Hamai, A. Greffard, V. Nicolas, P. Codogno, J. Botti, Autophagy modulates cell migration and beta1 integrin membrane recycling, Cell Cycle 12 (20) (2013) 3317–3328.

[32] M. Gugnoni, V. Sancisi, G. Manzotti, G. Gandolfi, A. Ciarrocchi, Autophagy and epithelial-mesenchymal transition: an intricate interplay in cancer, Cell Death Dis. 7 (12) (2016), e2520.
[33] P.-M. Wong, Y. Feng, J. Wang, R. Shi, X. Jiang, Regulation of autophagy by coordinated action of mTORC1 and protein phosphatase 2A, Nat. Commun. 6 (2015) 8048.
[34] C. Settembre, C. Di Malta, V.A. Polito, M. Garcia Arencibia, F. Vetrini, S. Erdin, S.U. Erdin, T. Huynh, D. Medina, P. Colella, et al., TFEB links autophagy to lysosomal biogenesis, Science (New York, NY) 332 (6036) (2011) 1429–1433.
[35] K.L. Bryant, C.A. Stalnecker, D. Zeitouni, J.E. Klomp, S. Peng, A.P. Tikunov, V. Gunda, M. Pierobon, A.M. Waters, S.D. George, et al., Combination of ERK and autophagy inhibition as a treatment approach for pancreatic cancer, Nat Med 25 (4) (2019) 628–640.
[36] C.G. Kinsey, S.A. Camolotto, A.M. Boespflug, K.P. Guillen, M. Foth, A. Truong, S.S. Schuman, J.E. Shea, M.T. Seipp, J.T. Yap, et al., Protective autophagy elicited by RAF→MEK→ERK inhibition suggests a treatment strategy for RAS-driven cancers, Nat Med 25 (4) (2019) 620–627.